Explicit Generalized Predictive Control of Speed and Position of PMSM Drives

Květoslav Belda and David Vošmik

***Abstract*—This paper deals with a specific explicit design of Generalized Predictive Control (GPC) for speed and position of three-phase Permanent Magnet Synchronous Motors (PMSM). Predictive algorithms are designed with single and double integrations with respect to step and ramp reference signals. Needful field weakening and current limitation are solved by specific procedures based on a local indirect tuning/amplification of the relevant GPC parameters. The proposed solution due to low computational demands is suitable for real applications. Designed algorithms and procedures are demonstrated by figures and oscillogram screenshots of representative variables measured on the 10.7 kW PMSM drive.**

***Index Terms*—Current limitation, field weakening, motion control, permanent magnet synchronous motors, position control, predictive control, speed control.**

I. Introduction

THREE-PHASE Permanent Magnet Synchronous Motors (PMSM) are now frequently applied to advanced electrical drives. Due to minor demands on maintenance and only few mechanical elements, those motors are used in many industrial applications (machine tools, robots-manipulators) and in many traffic applications (transport vehicles, trams, trolley-buses). Their control consists in the design of appropriate amplitude and phase of stator voltage entering Pulse-Width Modulation (PWM). PWM provides adequate amplitude and frequency of all Alternate Currents (AC) for the stator excitation.

A conventional approach is based on vector control realized by cascade configuration of PI controllers [1], [2]. That configuration represents a fixed coupling of separate PI controllers, where their mutual relations are considered as external disturbances. The cascade configuration consists of position, speed, and current loops with respect to the application. Usually, constant setting of PI controllers corresponds only to some specific working range without any optimization for changing motor states. It is a limitation for applications with the dynamically changeable working conditions and ranges.

A promising alternative is a model-based approach that naturally consider available information in the mathematical model. This approach consists in an optimization considering the model, user requirements, and physical constraints together.

Manuscript received May 31, 2015; revised October 20, 2015 and November 21, 2015; accepted December 20, 2015. Date of publication January 5, 2016; date of current version May 10, 2016.

K. Belda is with the Institute of Information Theory and Automation of the Czech Academy of Sciences, 182 08 Prague, Czech Republic (e-mail: belda@utia.cas.cz).

D. Vošmik is with the Regional Innovation Centre for Electrical Engineering, 306 14 Pilsen, Czech Republic (e-mail: vosmik1@rice.zcu.cz).

Color versions of one or more of the figures in this paper are available online at http://ieeexplore.ieee.org.

Digital Object Identifier 10.1109/TIE.2016.2515061

This paper focuses on Generalized Predictive Control (GPC) [3] as one advanced control strategy of the model-based approach. The GPC strategy [4] generally represents a complex multi-objective optimization, which can involve different control targets [5], [6], e.g., compliance with specific constraints or flexible setting of a controller stiffness. In this context, the GPC is considered as a suitable control design of PMSM drives with the same functionality and universality as the conventional control approach. However, model-based GPC approach is inherently more flexible and efficient. The aim of this paper is to introduce a straightforward GPC design as a fully equipped model-based continuous solution in comparison with widely used finite-set model predictive discrete solutions within specific regions as, e.g., in [2], [7], and [8].

This paper aims at fast explicit predictive control forms applied to the PMSM drives [9], [10]. The proposed GPC design is intended for the motion control, both speed control especially for traffic domain and position control for industrial robotics and machine tool applications. The suitability of the solution follows from its generality corresponding to the usual modern control theory [11].

The developed explicit forms employ fixed control laws with speed-variant gains. The gains are pre-computed offline for a given specific range of electrical rotor speed of the motor. The rotor speed represents only one selecting parameter that determines the unique values of a mathematical model of the considered motor for offline control gain calculation and values of the gains for online control action computation. The one parameter implies the fast real-time gain selection.

The designed algorithms realizing proposed explicit GPC are coupled with three front-end modules, which specifically adapt input signals entering the GPC algorithms. The modules, by a signal adaptation, enable GPC to solve a field weakening, current limitation, and coping with a known load torque. The known load is usually combined with position control, whereas other subtasks are predominantly employed in speed control. Stand-alone controllers based on developed algorithms and modules are demonstrated by real experiments on laboratory tandem of motors equipped with torque transducer between their shafts.

This paper is organized as follows. Section II outlines suitable mathematical models used for model-based control design. Section III introduces basic block diagram of predictive control. Section IV deals with front-end modules of GPC for torque-current control, field weakening, and current limitation. Section V explains the principles of explicit GPC algorithms. Section VI presents real experiments by figures and directly captured oscillogram screenshots.

II. Mathematical Models for Control Design

Models for speed and position control arise from the voltage distribution in the three AC phase system and from torque equilibrium equation [1]. Considering Clarke and Park transformation, the initial set of equations defined in d-q rotating field coordinate system or rotating reference frame is

$$u_{Sd} = R_S\, i_{Sd} + L_d \frac{d}{dt} i_{Sd} - L_q\, \omega_e\, i_{Sq} \tag{1}$$

$$u_{Sq} = R_S\, i_{Sq} + L_q \frac{d}{dt} i_{Sq} + L_d\, \omega_e\, i_{Sd} + \psi_M\, \omega_e \tag{2}$$

where R_S, L_d, L_q, and ψ_M are motor parameters, u_{Sd}, u_{Sq} are d-q voltages (system inputs), i_{Sd}, i_{Sq} are d-q currents, ω_e is the electrical rotor speed (mechanical speed $\omega_m = \omega_e/p$; p is a number of pole pairs),

$$J\frac{d^2}{dt^2}\vartheta_e = \frac{3}{2}p^2\,(\psi_M i_{Sq} + (L_d - L_q) i_{Sd} i_{Sq}) - B\,\omega_e - p\tau_L \tag{3}$$

where J and B are other motor parameters, ϑ_e is the electrical rotor position, and τ_L is a load torque. The model (1)–(3) can be rearranged into state-space models as follows (surface-mounted PMSM $L_d = L_q = L_S$ is considered):

- speed control with system output $y = [i_{S_d},\ i_{S_q},\ \omega_e]^T$

$$\frac{d}{dt}\begin{bmatrix} i_{Sd} \\ i_{Sq} \\ \omega_e \\ \tau_L \end{bmatrix} = \begin{bmatrix} -\frac{R_S}{L_S} & \omega_e & 0 & 0 \\ -\omega_e & -\frac{R_S}{L_S} & -\frac{\psi_M}{L_S} & 0 \\ 0 & \frac{3}{2}\frac{p^2}{J}\psi_M & -\frac{B}{J} & -\frac{p}{J} \\ 0 & 0 & 0 & 0 \end{bmatrix} \begin{bmatrix} i_{Sd} \\ i_{Sq} \\ \omega_e \\ \tau_L \end{bmatrix} + \begin{bmatrix} \frac{1}{L_S} & 0 \\ 0 & \frac{1}{L_S} \\ 0 & 0 \\ 0 & 0 \end{bmatrix} \begin{bmatrix} u_{Sd} \\ u_{Sq} \end{bmatrix} \tag{4}$$

- position control with system output $y = [i_{S_d},\ i_{S_q},\ \vartheta_e]^T$

$$\frac{d}{dt}\begin{bmatrix} i_{Sd} \\ i_{Sq} \\ \omega_e \\ \vartheta_e \\ \tau_L \end{bmatrix} = \begin{bmatrix} -\frac{R_S}{L_S} & \omega_e & 0 & 0 & 0 \\ -\omega_e & -\frac{R_S}{L_S} & -\frac{\psi_M}{L_S} & 0 & 0 \\ 0 & \frac{3}{2}\frac{p^2}{J}\psi_M & -\frac{B}{J} & 0 & -\frac{p}{J} \\ 0 & 0 & 1 & 0 & 0 \\ 0 & 0 & 0 & 0 & 0 \end{bmatrix} \begin{bmatrix} i_{Sd} \\ i_{Sq} \\ \omega_e \\ \vartheta_e \\ \tau_L \end{bmatrix} + \begin{bmatrix} \frac{1}{L_S} & 0 \\ 0 & 1\frac{1}{L_S} \\ 0 & 0 \\ 0 & 0 \\ 0 & 0 \end{bmatrix} \begin{bmatrix} u_{Sd} \\ u_{Sq} \end{bmatrix} \tag{5}$$

Both forms can be represented by one state-space model

$$\begin{aligned} \frac{d}{dt}\, x(t) &= A_c(\omega_e)\, x(t) + B_c\, u(t) \\ y(t) &= Cx(t) \end{aligned} \tag{6}$$

where $A_c(\omega_e)$ is a variable state-space matrix relative to ω_e, B_c is a constant input matrix, and C is a constant rectangular output matrix with unit elements in accord with output y. A set of the variables $[i_{Sd}, i_{Sq}, \omega_e, \tau_L]^T$ or $[i_{Sd}, i_{Sq}, \omega_e, \vartheta_e, \tau_L]^T$, respectively, represents state vector $x(t)$ of the motor. The two nonlinear terms $\omega_e\, i_{Sq}$ and $\omega_e\, i_{Sd}$ in (1) and (2) are decomposed in (4) and (5) according to a specific linearizing decomposition [12]. The state-space forms (4), (5) or their generalized expression (6) represent the initial models for model-based control design.

In this paper, a measurement of all state variables is assumed. However, the variables ϑ_e and ω_e may be estimated indirectly [1] (traffic systems), as well as the torque τ_L [13] (robotic systems). Torque τ_L can be determined for instance in compliance with torque equilibrium equation as

$$\hat{\tau}_L = \frac{3}{2}\, p\, \psi_M\, i_{Sq} - \frac{J}{p}\frac{d}{dt}\omega_e - \frac{B}{p}\,\omega_e. \tag{7}$$

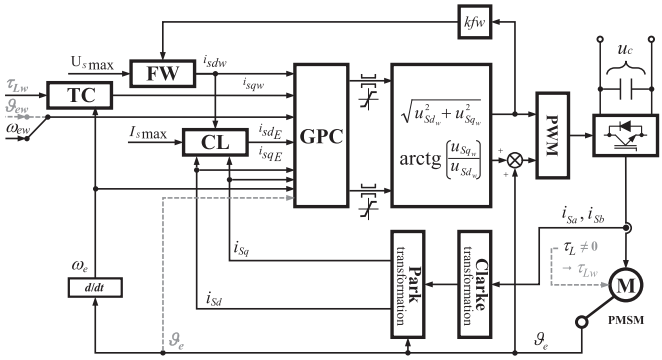

Fig. 1. Block diagram of Generalized Predictive Control that is applicable for speed and position control according to considered mathematical model (4) or (5) and appropriate inputs of the controller block GPC.

III. Basic Block Diagram

The predictive control in the basic block diagram (Fig. 1) is encapsulated in the one main block containing optimisation algorithms (off-line design) or predictive control laws with precomputed gains (on-line real use). This block is complemented by input-adapting modules of field weakening (FW), current limitation (CL), and reference torque-current conversion (TC), which will be described in Section IV. The block diagram is applicable for both considered tasks:

- speed control
  - ω_e is controlled toward its reference ω_{ew},
  - zero or negligible load torque τ_L is considered,
  - current components i_{Sd} and i_{Sq} are kept minimal;
- position control
  - ϑ_e is controlled toward its reference ϑ_{ew},
  - time-varying load torque τ_L is considered,
  - i_{Sd} is kept minimal and i_{Sq} toward $i_{Sqw} = f(\tau_{Lw})$.

The whole control circuit for speed and position control tasks contains at least one integrator for step reference signals or two integrators for ramp reference signals so that zero-steady-state error can be reached. The optimization, considering front-end blocks, uses all features of GPC design for all user control requirements or required reference signals:

- reference electrical rotor speed ω_{ew}
- field weakening at high speeds ω_e employing $i_{Sdw} \neq 0$ limited by $|i_{Sdw}| < I_{S\max}$
- current limitation complying with $\sqrt{i_{Sd}^2 + i_{Sq}^2} \leq I_{S\max}$
- reference electrical rotor position ϑ_{ew}
- reference output rotor torque τ_{Lw}.

The optimization procedure looks for a minimum amplitudes of control actions minimizing a used cost function that balances the user requirements with measured motor outputs and unknown control actions. GPC design principles, with computation algorithms will be explained in Section V.

IV. Front-End Modules

The front-end modules, TC, FW, and CL modules shown in Fig. 1, enable GPC design to prove comparable and compact set of functionalities as usual cascade control without increasing complexity of the design. TC module is needful if some nonzero reference torque τ_{Lw} is required. FW and CL modules are necessary for the limiting cases of high values of the speed and abrupt current peaks.

The requirement on complying with the reference torque can be solved via equilibrium torque equation. Field weakening can be achieved by adjustment of the flux current component [1]. The remaining current limitation problem can be solved inside as a part of GPC global optimization, e.g., via a quadratic programming [11]. However, such usual solution leads to the algorithms unfeasible in real time in view of PMSM dynamics. Different ways consist in the direct penalization of possible current overshoots evaluated for a limited set of predictions within short prediction horizons [13], [14]. Similar idea will be considered here. However, the proposed solution will be involved into a usual GPC design without any restriction on a prediction horizon length.

The resulting solution of mentioned problems will take part of a cost function optimization by a specific on-line excitation of the inputs adapted by front-end modules. It represents a specific indirect local amplification of the appropriate weight parameters of GPC cost functions considered in the optimization of the appropriate control actions.

A. TC Module

TC module arises from torque equilibrium equation (3). The module represents only a simple rearrangement of this equation

$$i_{Sqw} = \frac{2}{3}\,\frac{1}{p^{\,2}\,\psi_M}\,\left(p\,\tau_{Lw} + J\,\frac{d}{dt}\,\omega_{ew} - B\,\omega_{ew}\right). \tag{8}$$

Equation (8) represents in fact a conversion of the known torque reference τ_{Lw} into reference of the q-current component i_{Sqw} that is simply processable in control design as a standard reference input.

B. FW Module

Field weakening is necessary if a further increase of the rotor speed is required and supply voltage cannot be increased onward in appropriate way, just due to voltage supply limits. Since the direct control of magnetic flux Ψ_M is not possible with respect to permanent magnets, the field weakening is provided by incorporating a negative d-current (flux) component i_{Sd} [1]. The adjustment of i_{Sd} is limited by the following condition:

$$i_S = \sqrt{i_{Sd}^2 + i_{Sd}^2} \le I_{S\max} \tag{9}$$

where $I_{S\max}$ is a maximum admissible stator current of the motor.

The described idea can be used in similar way in GPC design. The adjustment of the d-current component represents a new specific reference value i_{Sdw} that is negative, if the weakening property is necessary, otherwise is zero. The FW module preceding GPC block is based on this principle. Its procedure can be expressed as follows:

$$\begin{aligned}
&u_S := \sqrt{u_{Sd}^2 + u_{Sd}^2};\\
&\text{if } u_S \ge U_{S\max},\\
&\quad i_{Sdw} := (U_{S\max} - u_S)\,k_{fw};\\
&\quad \text{if } |i_{Sdw}| > I_{S\max},\ i_{Sdw} := -I_{S\max}\,k_{i_{ub}};\ \text{end}\\
&\text{else}\\
&\quad i_{Sdw} := 0;\\
&\text{end}
\end{aligned} \tag{10}$$

This procedure gives nonzero reference i_{Sdw} (first if-block) and reduces its possible overshoot of $I_{S\max}$ (second if-block).

C. CL Module

Current limitation is important for a safe use of PMSM drives. The current sum may not exceed admissible stator current $I_{S\max}$; otherwise, current overshoot can cause a drive malfunction or activation of current breakers leading to an undesirable drive operation interruption. The procedure of the CL module boosts the magnitudes of d-q current components to increase their weight greatly in the appropriate cost function during its optimization in GPC design or in a precomputed explicit control law. It can be given as follows:

$$\begin{aligned}
&i_{SdE} := i_{Sd};\\
&i_{SqE} := i_{Sq};\\
&\text{if } |i_{Sq}| \ge \sqrt{I_{S\max}^2 - i_{Sdw}^2},\ i_{SqE} := \left(\frac{|i_{Sq}|}{I_{S\max}}\right)^{k_{sp}} i_{Sq};\\
&\text{else if } |i_{Sd}| > I_{S\max}\,k_{i_{ub}},\ i_{SdE} := \left(\frac{|i_{Sd}|}{I_{S\max}}\right)^{k_{sp}} i_{Sd};\\
&\text{end}
\end{aligned} \tag{11}$$

where $k_{\rm sp}$ is a suitably selected exponent, and currents i_{SdE} and i_{SqE} are modified inputs of GPC.

Outlined procedure causes that the appropriate real current components will be intensively suppressed by weighting matrices in appropriate design cost function or GPC control law. Thus, artificial proportional extension of appropriate current component appears as a big outlier against other function terms and a predictive control law strongly suppresses such outlier. From practical point of view, the changeable lower limit $\sqrt{\left(I_{S\max}^2 - i_{S\rm dw}^2\right)}$ in (11) is reasonable to be held above some meaningful level so that the condition would be feasible. The proposed procedure (11) gives acceptable results, but it does not represent hard limitation. It is only soft limitation, which comes close to hard limitation.

From GPC design point of view, the proposed algorithms (10) and (11) including (8) do not change a control design complexity or tuning of control parameters. The algorithms only modify selected inputs to the GPC controller. In fact, it means a specific indirect local tuning of control parameters that are inseparable with the signals in appropriate products.

V. Principles of GPC Algorithms

A. Preliminaries of Predictive Control Design

This section outlines essential design terms and key procedural steps of the design. A used notation considers several principal variables

$$\Delta x, \quad x, \quad \Delta y, \quad y, \quad \Delta u, \quad u, \quad e, \quad w.$$

All variables are considered and defined as vectors respecting general multidimensional definition. They represent increments and absolute values of the system state, system outputs, control actions, errors, and references. Their definitions and utilization in GPC design will be introduced in the subsequent sections that deal with a specific composition of the equations of predictions, used quadratic cost functions, and adapted minimization control laws for control actions.

The GPC algorithms are derived as discrete (digital) procedures suitable for a usual digital implementation. They provide computation of control actions within one optimization calculation. Generally, the calculation employs predictions of expected future output values mathematically expressed by equations of predictions [3]. These equations are closely related to the form of a cost function [15]. As mentioned, at a predictive control design, the quadratic cost function is used in various forms. A particular form depends on used equations of predictions that correspond to required control targets. In this paper, the two specific forms are introduced. They differ in the number of included integrators. Their features correspond to the conventional cascade configuration.

B. Composition of Equations of Predictions

The equations of predictions express the functions of future system outputs in relation to unknown future control actions. The composition of the equations is always initiated by a discretization of updated state-space model (6) considering current ω_e. A consequent discrete state-space model is as follows:

$$\begin{aligned} \hat{x}_{k+1} &= A\, x_k + B\, u_k \\ y_k &= C\, x_k \end{aligned} \tag{12}$$

where $A = A_k(\omega_{e\,(k)}) = A_{k+i}$, $i = 1, \ldots, N$ for an optimization in the current time instant k along a current prediction horizon N. The next optimization in the instant $k+1$ is initiated by update of model (6) and its discretization again. In addition to the discrete model (12), an evolution model of aggregated control error $\bar{e}_k$ is taken into account

$$e_k = w_k - y_k, \; \bar{e}_k = \bar{e}_{k-1} + e_k. \tag{13}$$

To achieve integral property in the design, the model (12) can be written in an incremental form in the following way:

$$\begin{aligned} \hat{x}_{k+1} - x_k &= A\,(x_k - x_{k-1}) + B\,(u_k - u_{k-1}) \\ \hat{y}_{k+1} - y_k &= C\,(x_k - x_{k-1}) \end{aligned} \tag{14}$$

and in a condensed incremental form as well

$$\begin{aligned} \Delta\hat{x}_{k+1} &= A\,\Delta x_k + B\,\Delta u_k \\ \Delta\hat{y}_{k+1} &= C\,\Delta x_k. \end{aligned} \tag{15}$$

The model (15) represents the base of the incremental feature of the equations of predictions used in the proposed predictive control design. The sequence of their composition corresponds to the cost functions in Sections V-C and V-D.

The procedures of the composition are based on recursive principle. It is involved in the initial equations (16), (17), (20), and (23) by the index $j = 1, \ldots, N$ that determines individual discrete time instants for the prediction horizon N.

The mentioned equations are defined as follows. Equation (16) is for predictions of the system state increments $\Delta\hat{x}$

$$\Delta\hat{x}_{k+j} = A^j\,\Delta x_k + \sum_{i=1}^{j} A^{i-1} B \Delta u_{k+j-i}. \tag{16}$$

Equation (17) defines increments of system outputs $\Delta\hat{y}$

$$\Delta\hat{y}_{k+j} = CA^j\,\Delta x_k + \sum_{i=1}^{j} CA^{i-1} B \Delta u_{k+j-i}. \tag{17}$$

It can be written in the condensed matrix form (18)

$$\Delta\hat{Y} = F_1\,\Delta x_k + G_1\,\Delta U \tag{18}$$

where individual elements $\Delta\hat{Y}$, ΔU, F_1, and G_1 are as follows:

$$\begin{aligned} \Delta\hat{Y} &= [\,\Delta\hat{y}_{k+1}^T \;\cdots\; \Delta\hat{y}_{k+N}^T\,]^T \\ \Delta U &= [\,\Delta u_k^T \;\cdots\; \Delta u_{k+N-1}^T\,]^T \\ F_1 &= \begin{bmatrix} CA \\ \vdots \\ CA^N \end{bmatrix}, \; G_1 = \begin{bmatrix} CB & \cdots & 0 \\ \vdots & \ddots & \vdots \\ CA^{N-1}B & \cdots & CB \end{bmatrix}. \end{aligned} \tag{19}$$

Equation (20) represents evolution of the full-value predictions of the system outputs $\hat{y}$

$$\hat{y}_{k+j} = y_k + \sum_{i=1}^{j} \Delta\hat{y}_{k+i}. \tag{20}$$

The appropriate matrix notation of (20) is the following:

$$\hat{Y} = F_{\mathrm{I}}\, y_k + F_2\,\Delta x_k + G_2\,\Delta U \tag{21}$$

where subsequent individual elements $\hat{Y}$, F_{I}, F_2, and G_2 are defined as

$$\begin{aligned} \hat{Y} &= [\,\hat{y}_{k+1}^T \;\cdots\; \hat{y}_{k+N}^T\,]^T \\ F_{\mathrm{I}} &= [\,I \;\cdots\; I\,]^T \\ F_2 &= \begin{bmatrix} CA \\ \vdots \\ \sum_{i=1}^{N} CA^i \end{bmatrix}, G_2 = \begin{bmatrix} CB & \cdots & 0 \\ \vdots & \ddots & \vdots \\ \sum_{i=1}^{N} CA^{i-1}B & \cdots & CB \end{bmatrix}. \end{aligned} \tag{22}$$

Finally, equation (23) is for an aggregate control error $\hat{\bar{e}}$

$$\begin{aligned} \hat{\bar{e}}_{k+j-1} = \bar{e}_k &+ \sum_{i=1}^{j-1} \{w_{k+i}\} - (j-1)\, I\, y_k \\ &- \sum_{i=1}^{j-1} \{(j-i) C\, A^i\}\;\Delta x_k \\ &+ \sum_{i=1}^{j-1} \left\{ \sum_{l=1}^{j-1} \{(j-i) C\, A^{i-l} B\}\, \Delta u_{k+l-1} \right\}. \end{aligned} \tag{23}$$

Equation (23) can be expressed, as well as previous equations, in the following matrix form:

$$\hat{E} = F_{\mathrm{I}}\,\bar{e}_k + W_s - F_{\mathrm{II}}\,y_k - F_3\,\Delta x_k - G_3\,\Delta U \tag{24}$$

where remaining elements $\hat{E}$, W_s, F_{II}, F_3, and G_3 are

$$\hat{E} = [\,\bar{e}_k^T\ \ \hat{\bar{e}}_{k+1}^T\ \ \hat{\bar{e}}_{k+2}^T\ \cdots\ \hat{\bar{e}}_{k+N-1}^T\,]^T$$

$$W_s = \left[\,0^T w_{k+1}^T (w_{k+1}+w_{k+2})^T\ \cdots\ \left(\sum_{i=1}^{N-1}\{w_{k+i}\}\right)^T\,\right]^T$$

$$F_{\mathrm{II}} = [\,0\ \ I\ \ 2I\ \cdots\ (N-1)\,I\,]^T$$

$$F_3 = \left[\,0^T\ \ (CA)^T(2CA+CA^2)^T\ \cdots\ \left(\sum_{i=1}^{N-1}(N-i)CA^i\right)^T\,\right]^T$$

$$G_3 = \begin{bmatrix} 0 & \cdots & 0 & 0 & 0 \\ CB & \cdots & 0 & 0 & 0 \\ \vdots & & \ddots & \vdots & \vdots \\ \sum_{i=1}^{N-1}(N-i)CA^{i-1}B & \cdots & 2CB+CAB & CB & 0 \end{bmatrix}. \tag{25}$$

C. GPC with Single Integrator (First GPC Algorithm)

Let us consider a quadratic cost function in the form

$$\begin{aligned} J_k &= \sum_{j=1}^{N} \{\|(\hat{y}_{k+j} - w_{k+j})\,Q_{yw}\|_2^2 \\ &\quad + \|\Delta\hat{y}_{k+j}\,Q_{\Delta y}\|_2^2 + \|\Delta u_{k+j-1}\,Q_{\Delta u}\|_2^2\} \\ &= (\hat{Y}-W)^T Q_{YW}(\hat{Y}-W) \\ &\quad + \Delta\hat{Y}^T Q_{\Delta Y}\Delta\hat{Y} + \Delta U^T Q_{\Delta U}\Delta U \end{aligned} \tag{26}$$

where W, Q_{YW}, $Q_{\Delta Y}$, and $Q_{\Delta U}$ are defined as

$$W = [\,w_{k+1}^T\ \ w_{k+2}^T\ \cdots\ w_{k+N}^T\,]^T$$

$$Q_\diamond = \left[\begin{matrix} Q_*^T Q_* & & 0 \\ & \ddots & \\ 0 & & Q_*^T Q_* \end{matrix}\right] \left|\begin{array}{l} \text{subscripts } \diamond, * : \\ \diamond \in \{YW,\ \Delta Y,\ \Delta U\} \\ * \in \{yw,\ \Delta y,\ \Delta u\}. \end{array}\right. \tag{27}$$

The minimization of the function (26) by searching for its local minimum leads to the control law (28)

$$\begin{aligned} \Delta u_k = M(&G_2^T Q_{YW} G_2 + G_1^T Q_{\Delta Y} G_1 + Q_{\Delta U})^{-1} \\ &\times \left[G_2^T Q_{YW}(W - F_{\mathrm{I}} y_k)\right. \\ &\left. - \left\{G_2^T Q_{YW} F_2 + G_1^T Q_{\Delta Y} F_1\right\}\Delta x_k\,\right] \end{aligned} \tag{28}$$

where a rectangular matrix M is a matrix, which selects the appropriate first rows of control action increments $\Delta u_k = M\Delta U$ corresponding to the current time instant k.

To simplify the computation, $w_{k+j} = w_k$ for $j = 1, \ldots, N$ can be considered with regard to a fast dynamics of PMSM drives. Then, the algorithm with integration of Δu and penalization of output increments Δy will be composed as follows:

$$\begin{aligned} e_k &:= w_k - y_k \\ \Delta x_k &:= x_k - x_{k-1} \\ \Delta u_k &:= K_e F_{\mathrm{I}} e_k - K_{\Delta x}\Delta x_k \\ u_k &:= u_{k-1} + \Delta u_k. \end{aligned} \tag{29}$$

Individual matrix gains K_e and $K_{\Delta x}$ in (29) are precomputed off-line for whole range of ω_e. During a control process, they are only selected by current ω_e. The gains correspond to the itemized form of the control law (28) as follows:

$$\begin{aligned} K_e &= M(\cdot)^{-1} \times G_2^T Q_{YW} \\ K_{\Delta x} &= M(\cdot)^{-1} \times \{\cdot\}. \end{aligned} \tag{30}$$

D. GPC with Double Integrator (Second GPC Algorithm)

Let us consider another form of the quadratic cost function

$$\begin{aligned} J_k &= \sum_{j=1}^{N} \{\|(\hat{y}_{k+j} - w_{k+j} - \hat{\bar{e}}_{k+j-1})\,Q_{yw}\|_2^2 \\ &\quad + \|\Delta\hat{y}_{k+j}\,Q_{\Delta y}\|_2^2 + \|\Delta u_{k+j-1}\,Q_{\Delta u}\|_2^2\} \\ &= \left(\hat{Y} - W - \hat{E}\right)^T Q_{YW}\left(\hat{Y} - W - \hat{E}\right) \\ &\quad + \Delta\hat{Y}^T Q_{\Delta Y}\Delta\hat{Y} + \Delta U^T Q_{\Delta U}\Delta U. \end{aligned} \tag{31}$$

The minimization of the function (31) by searching for the local minimum leads to the following control law (32):

$$\begin{aligned} \Delta u_k = M(&G^T Q_{YW} G + G_1^T Q_{\Delta Y} G_1 + Q_{\Delta U})^{-1} \\ &\times \left[\,G^T Q_{YW}\bar{e}_k + G^T Q_{YW} W + G^T Q_{YW} W_s\right. \\ &- G^T Q_{YW}(F_{\mathrm{I}} + F_{\mathrm{II}})y_k \\ &\left. - \left\{G_2^T Q_{YW}(F_2 + F_3) + G_1^T Q_{\Delta Y} F_1\right\}\Delta x_k\,\right] \end{aligned} \tag{32}$$

where $G = G_2 + G_3$.

To simplify the computation, the references $w_{k+j} = w_k$ for $j = 1, \ldots, N$ can be considered as well as in the previous first algorithm. Then, the algorithm with integration of Δu and $\bar{e}$ including penalization of output increments Δy will be composed as follows:

$$\begin{aligned} e_k &:= w_k - y_k \\ \bar{e}_k &:= \bar{e}_{k-1} + e_k \\ \Delta x_k &:= x_k - x_{k-1} \\ \Delta u_k &:= K_e\,\bar{e}_k + K_e F_{\mathrm{I}} w_k + K_e F_{\mathrm{II}} w_k \\ &\quad - K_y y_k \\ &\quad - K_{\Delta x}\Delta x_k \\ u_k &:= u_{k-1} + \Delta u_k. \end{aligned} \tag{33}$$

Individual matrix gains K_e, K_y, and $K_{\Delta x}$ in (33) are precomputed off-line. Then, in a control process, they are only selected by particular current ω_e as well. The gains correspond to the itemized form of the control law (32) as follows:

$$\begin{aligned} K_e &= M(\cdot)^{-1} \times G^T Q_{YW} \\ K_y &= K_e(F_{\mathrm{I}} + F_{\mathrm{II}}) \\ K_{\Delta x} &= M(\cdot)^{-1} \times \{\cdot\}. \end{aligned} \tag{34}$$

Note that if current limitation and field weakening conditions are activated, then appropriate current elements of vectors y_k and w_k in the first algorithm with single integrator (29) or in the second algorithm with double integrator (33) are replaced by modified, adapted inputs $y_{k(1:2,1)} = [i_{SdE},\ i_{SqE}]^T$ and $w_k = [i_{Sdw}, i_{Sqw}, \omega_{ew}]^T$ or $w_k = [i_{Sdw}, i_{Sqw}, \vartheta_{ew}]^T$ according to selected control task and appropriate procedures described in Sections III and IV, respectively.

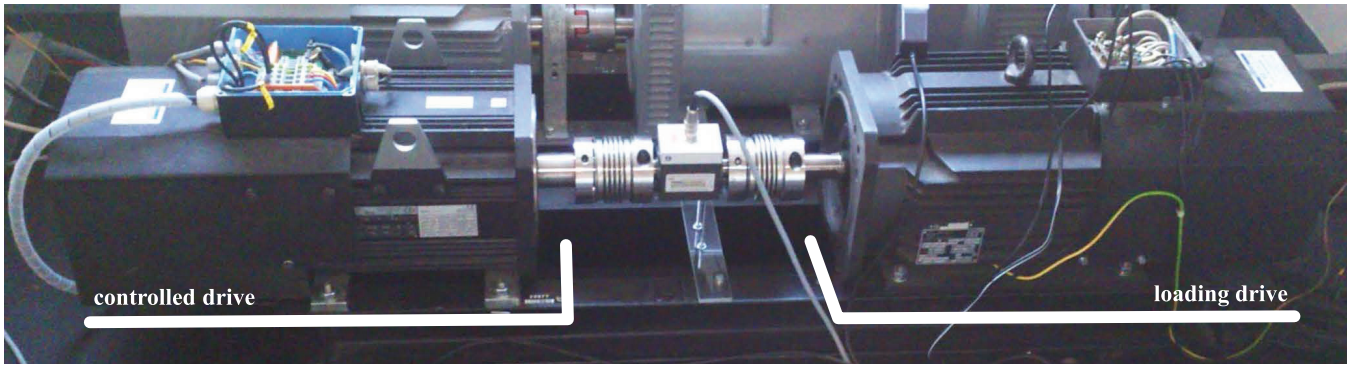

Fig. 2. Testing stand: controlled PMSM drive −10.7 kW, torque transducer (middle), and coupled loading induction motor drive −14.5 kW.

VI. Real Experiments

This section demonstrates the proposed algorithms implemented in the control system based on DSP TMS320f28335. The control system is connected to the laboratory PMSM drive of rated power 10.7 kW and to the torque transducer T20WN/100NM. The main parameters of the motor are listed in the Table I at the end of this section. The testing stand with PMSM drive, torque transducer, and coupled loading motor is shown in Fig. 2.

The optimal gains employed in control laws of GPC algorithms (29) or (33) are tuned and computed offline by computer simulation for whole admissible range of the parameter ω_e. The values of the individual elements of the gains are stored as fixed interpolating functional approximations, which follow their trends for considered admissible ω_e range [9]. The trends of absolute values of the gains are symmetric with vertical symmetry axis $\omega_e = 0$. It simplifies the storing of gain values. As an example, the representative trends for matrix gain K_e are plotted in Fig. 3.

During real control experiments, the gains are only selected from the approximations just according to current ω_e. Thus, the control actions are computed with front-end modules TC, FW, and CL and explicit control algorithms (29) or (33) including continuously changed gains. The computation is fast and achievable at considered sampling $Ts = 125\,\mu s$ (8 kHz).

The algorithms (29) or (33) are applicable to both speed and position PMSM control tasks, just the relevant gain variables, signals, and reference values have to be properly selected with respect to models (4) and (5).

The representative illustrations of the experiments include:

- speed control
  - slow high triangular speed signal ω_{ew} (Fig. 4) with parameters in columns (A);
  - fast low triangular speed signal ω_{ew} (Fig. 5) with the parameters in columns (B);

  where (A) and (B) are columns of the Tables II and III.
- position control
  - position step signal ϑ_{ew} (Fig. 6);
  - position sine signal ϑ_{ew} (Fig. 7);

  both for zero load (left) and changing load (right) with parameters listed in the Table IV.

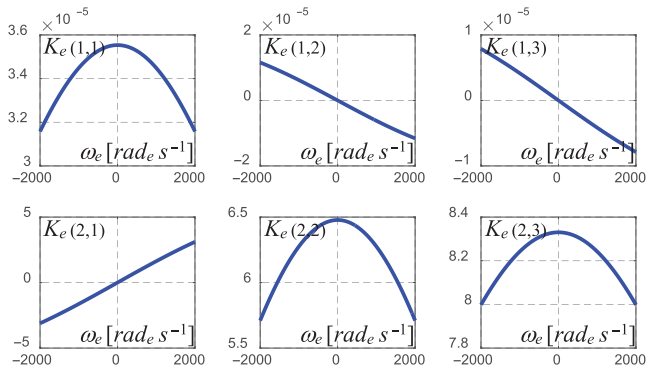

Fig. 3. Example of trends for elements of the gain $K_e = f(\omega_e)$ in (29).

Fig. 4 demonstrates the algorithms when high triangular speed profile is required. Speed reference profile passes through field weakening region bounded approximately by 900 rpm. The proposed GPC algorithms, bounded by current I_{smax}, ensure reliable function in full speed operating range. The first algorithm slowly drifts from the reference slope. It is caused by only one integrator involved in the algorithm. The second algorithm follows ramp segments more closely owing to double integrator. The both algorithms cannot solve speed error fully under field weakening and current limitation that are caused by excessive requirements of high command speed $\omega_{ew} = \pm 2000$ rpm but insufficient (limited) power input.

Fig. 5 shows proposed GPC algorithms at fast low triangular speed reference signal. It is evident that double integrator (second algorithm) has positive influence. For triangular or ramp reference signals, the asymptotic tracking of the second algorithm is obvious unlike the first algorithm with a steady offset. It corresponds to different behaviour of q-current components. The second algorithm shows sharper current slopes, rectangular-like shape of i_{Sq} signal. Since no field weakening is appeared, the needful i_{Sq} current can be used for the motion.

Finally, Figs. 6 and 7 demonstrate the behavior of the first GPC algorithm for positional motion control. In the figures on the left, a control process is uniform with zero load, whereas on the right, the process is influenced by nonzero load that is manually switched (load sw.) from +13.4 Nm to −11.5 Nm with manually switched controller ahead (controller sw.) so that the switch would be perceptible.

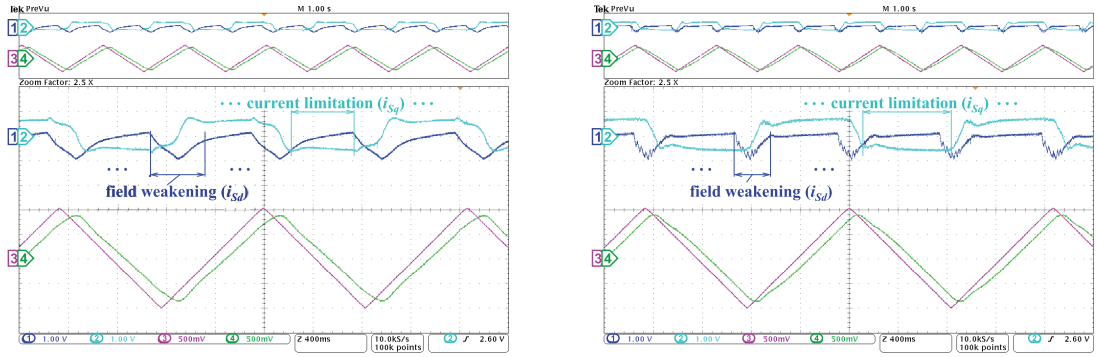

Fig. 4. Speed control: comparison of the first (left) and second (right) GPC algorithms for high triangular command speed ±2000 rpm; ch1: i_{Sd} current (25 A/1 V), ch2: i_{Sq} current (25 A/1 V), ch3: ω_{ew} command el. rotor speed (135 Hz/1 V), ch4: ω_e measured el. rotor speed (135 Hz/1 V) .

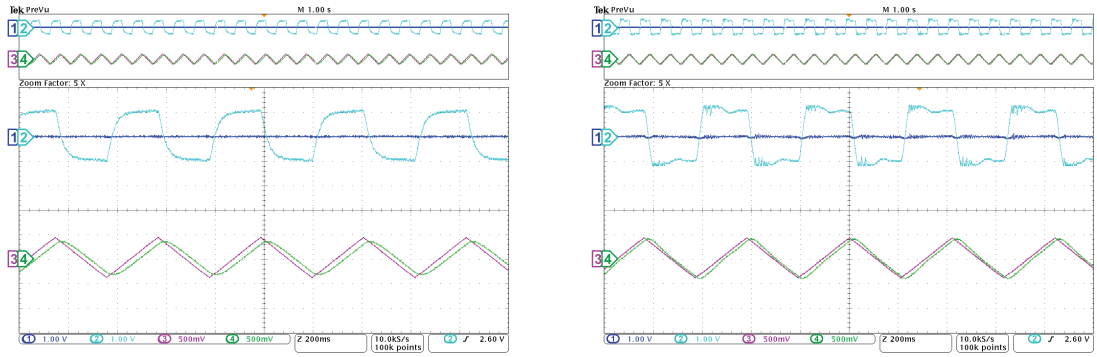

Fig. 5. Speed control: comparison of the first (left) and second (right) GPC algorithms for low triangular command speed ±800 rpm; ch1: i_{Sd} current (25 A/1 V), ch2: i_{Sq} current (25 A/1 V), ch3: ω_{ew} command el. rotor speed (135 Hz/1 V), ch4: ω_e measured el. rotor speed (135 Hz/1 V).

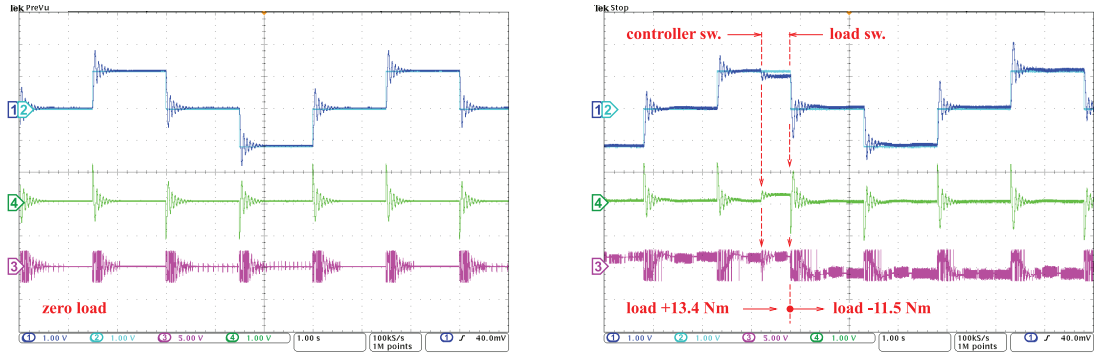

Fig. 6. Position control: comparison of the first GPC algorithm for step signal ($[0, +1.5, 0, -1.5, 0]$ rad$_e$) with zero load (left) and changing load (right); ch1: ϑ_e (1.256 rad$_e$/1 V), ch2: ϑ_{ew} (1.256 rad$_e$/1 V), ch3: i_{Sq} current (8 A/1 V), ch4: $\vartheta_{ew} - \vartheta_e$ (1.256 rad$_e$/1 V).

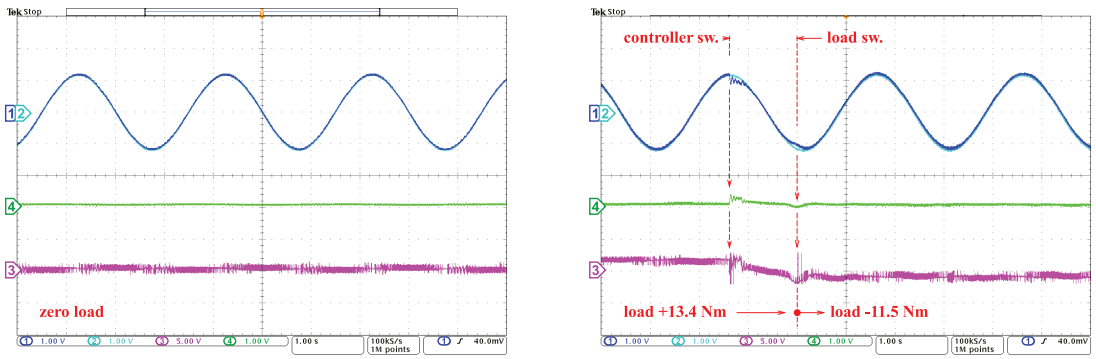

Fig. 7. Position control: comparison of the first GPC algorithm for sine signal (amplitude ±1.5 rad$_e$) with zero load (left) and changing load (right); ch1: ϑ_e (1.256 rad$_e$/1 V), ch2: ϑ_{ew} (1.256 rad$_e$/1 V), ch3: i_{Sq} current (8 A/1 V), ch4: $\vartheta_{ew} - \vartheta_e$ (1.256 rad$_e$/1 V).

TABLE I
PARAMETERS OF THE EMPLOYED PMSM DRIVE

Symbol	Description	Value
P	Rated power	10.7 kW
R_S	Stator resistance	0.28 Ω (Ohm)
L_S	Stator inductance	0.003465 H (Henry)
Ψ_M	PM rotor magnetic flux	0.1989 Wb (Weber)
B	Viscous friction coef.	0 kg m^2 s^{-1}
p	Number of pole pairs	4
J	Moment of inertia	0.04 kg m^2

TABLE II
SPEED CONTROL: PARAMETERS OF THE FIRST GPC ALGORITHM

Symbol	Description	Value (A)	Value (B)
N	Horizon of prediction	4	
Q_{yw}	Output penalization	diag(2, 1, 2)	diag(2, 1, 2)
$Q_{\Delta y}$	Output incr. penalization	diag(10^2, 20, 2)	diag(20, 80, 5)
$Q_{\Delta u}$	Input incr. penalization	diag(14, 7)	diag(5, 3.5)
Ts	Sampling period	0.000125 s	
k_{fw}	Field weakening gain	10^4	
ki_{ub}	Margin coefficient	0.9	
ksp	Current lim. exponent	40	

TABLE III
SPEED CONTROL: PARAMETERS OF THE SECOND GPC ALGORITHM

Symbol	Description	Value (A)	Value (B)
N	Horizon of prediction	4	
Q_{yw}	Output penalization	diag(10, 5, 4)	diag(10, 5, 10)
$Q_{\Delta y}$	Output incr. penalization	diag(140, 80, 1)	diag(20, 80, 1)
$Q_{\Delta u}$	Input incr. penalization	diag(20, 8)	diag(10, 8)
Ts	Sampling period	0.000125 s	
k_{fw}	Field weakening gain	4×10^4	
ki_{ub}	Margin coefficient	0.9	
ksp	Current lim. exponent	100	50

TABLE IV
POSITION CONTROL: PARAMETERS OF THE BOTH GPC ALGORITHMS

Symbol	Description	Value
N	Horizon of prediction	10
Q_{yw}	Output penalization	diag(10^{-2}, 10^{-2}, 5)
$Q_{\Delta y}$	Output incr. penalization	diag(10^{-3}, 10^{-2}, 600)
$Q_{\Delta u}$	Input incr. penalization	diag(10^{-3}, 10^{-3})
Ts	Sampling period	0.000125 s

Fig. 6 shows the sharp motion control along position steps $\vartheta_{ew} \in [0, -1.5, 0, +1.5, 0]$ rad$_e$, which correspond to mechanical turns ± 21.5 deg$_m$. The sharp ϑ_{ew} steps serve as a testing boundary reference signals with respect to a robotic application intension of motion control. Smooth reference signals are usually dominant in motion control, thus sine reference is used additionally. Fig. 7 demonstrates self-possessed GPC control along a sine reference signal with amplitude ± 1.5 rad$_e$ $\approx \pm 21.5$ deg$_m$ as for the step signal in Fig. 6. The reference positions ϑ_{ew} (step and sine signals) are continuously followed by real rotor position ϑ_e that converges to zero control error both for zero and changing load. In practice the motion control usually works with smooth trajectories, acceleration, deceleration as well as real load torques are without a sign alteration against shown experiments, especially in Fig. 6.

VII. CONCLUSION

This paper has presented novel algorithms of model-based predictive control [15] as an alternative to the conventional cascade control [1]. Real experiments on laboratory 10.7 kW PMSM drive demonstrate a flexibility of the proposed algorithms under various working conditions. Fast responses of the algorithms (8 kHz) follow from the explicit GPC formulation enabling off-line precomputation and fast selection of control law gains according to only one parameter. Thus, the proposed algorithms have an evident potential for future development in PMSM motion control.

REFERENCES

[1] P. Vas, *Sensorless Vector and Direct Torque Control*. London, U.K.: Oxford Univ. Press, 1998.

[2] H. Guzman *et al.*, "Comparative study of predictive and resonant controllers in fault-tolerant five-phase induction motor drives," *IEEE Trans. Ind. Electron.*, vol. 63, no. 1, pp. 606–617, Jan. 2016.

[3] A. Ordys and D. Clarke, "A state-space description for GPC controllers," *Int. J. Syst. Sci.*, vol. 24, no. 9, pp. 1727–1744, 1993.

[4] S. Vazquez *et al.*, "Model predictive control," *IEEE Ind. Electron. Mag.*, vol. 8, no. 1, pp. 16–31, Mar. 2014.

[5] K. Belda, "On-line solution of system constraints in generalized predictive control design," in *Proc. Int. Conf. Process Control*, 2015, pp. 25–30.

[6] P. Serkies and K. Szabat, "Application of the MPC to the position control of the two-mass drive system," *IEEE Trans. Ind. Electron.*, vol. 60, no. 9, pp. 3679–3688, Sep. 2013.

[7] T. Zanma, M. Kawasaki, K. Liu, M. Hagino, and A. Imura, "Model predictive direct torque control for PMSM with discrete voltage vectors," *IEEJ J. Ind. Appl.*, vol. 3, no. 2, pp. 121–130, 2014.

[8] E. Fuentes, D. Kalise, J. Rodriguez, and R. Kennel, "Cascade-free predictive speed control for electrical drives," *IEEE Trans. Ind. Electron.*, vol. 61, no. 5, pp. 2176–2184, May 2014.

[9] K. Belda and D. Vošmik, "Explicit GPC algorithms for speed control of PMSM drives," in *Proc. Annu. Conf. IEEE Ind. Electron. Soc. (IECON)*, Vienna, Austria, 2013, pp. 2833–2838.

[10] W. Xie *et al.*, "FCS model predictive torque control with a deadbeat solution for PMSM drives," *IEEE Trans. Ind. Electron.*, vol. 62, no. 9, pp. 5402–5410, Sep. 2015.

[11] J. Maciejowski, *Predictive Control With Constraints*. Englewood Cliffs, NJ, USA: Prentice-Hall, 2002.

[12] K. Belda, "Mathematical modelling and predictive control of PMSM drives," *Trans. Elect. Eng.*, vol. 2, no. 4, pp. 114–120, 2013.

[13] M. Lopez, J. Rodriguez, C. Silva, and M. Rivera, "Predictive torque control of a multidrive system fed by a dual indirect matrix converter," *IEEE Trans. Ind. Electron.*, vol. 62, no. 5, pp. 2731–2741, May 2015.

[14] A. Formentini *et al.*, "Speed finite control set model predictive control of a PMSM fed by matrix converter," *IEEE Trans. Ind. Electron.*, vol. 62, no. 11, pp. 6786–6796, Nov. 2015.

[15] L. Wang, *Model Predictive Control System Design*. New York, NY, USA: Springer, 2009.

Květoslav Belda received the M.Sc. degree in automatic control and engineering informatics, the Ph.D. degree in technical cybernetics, and the second Ph.D. degree in electrical engineering and informatics from the Czech Technical University in Prague, Prague, Czech Republic, in 1999, 2003, and 2006, respectively.

Since 1999, he has been a Researcher with the Institute of Information Theory and Automation of the CAS. His research interests include model-based control design, drives, industrial robotics, and mechatronics.

David Vošmik received the M.Sc. degree in electrical engineering and the Ph.D. degree in electronics from the University of West Bohemia, Pilsen, Czech Republic, in 2006 and 2014, respectively.

He is a member of the Regional Innovation Centre for Electrical Engineering (RICE), Pilsen, Czech Republic. His research interests include power electronics and drives, including parameter identification and signal estimation.